



Load Frequency Control in Power Systems Using Multi Objective Genetic Algorithm & Fuzzy Sliding Mode Control

M. Khosraviani¹, M. Jahanshahi², M. Farahani³, A.R. Zare Bidaki⁴

¹ Department of Computer Engineering. and IT, Islamic Azad University, Parand, Tehran, Iran, mkhosraviani@aut.ac.ir

² Department of Computer Engineering, Central Tehran Branch, Islamic Azad University, Tehran, Iran, mjahanshahi@iauctb.ac.ir

³ Young Researchers and Elite Club, East Tehran Branch, Islamic Azad University, Tehran Iran, m.farahani@basu.ac.ir

⁴ Young Researchers and Elite Club, Buinzahra Branch, Islamic Azad University, Buinzahra, Iran, azare@buiniau.ac.ir

Abstract

This study proposes a combination of a fuzzy sliding mode controller (FSMC) with integral-proportion-Derivative switching surface based superconducting magnetic energy storage (SMES) and PID tuned by a multi-objective optimization algorithm to solve the load frequency control in power systems. The goal of design is to improve the dynamic response of power systems after load demand changes. In the proposed method, an adaptive fuzzy controller is utilized to mimic a feedback linearization control law. To compensate the compensation error between the feedback linearization and adaptive fuzzy controller, a hitting controller is developed. The Lyapunov stability theory is used to obtain an adaption law so that the closed-loop system stability can be guaranteed. The optimal PID controller problem is formulated into a multi-objective optimization problem. A Pareto set of global optimal solutions to the given multi-objective optimization problem is generated by a genetic algorithm (GA)-based solution technique. The best compromise solution from the generated Pareto solution set is selected by using a fuzzy-based membership value assignment method. Simulations are presented and compared with conventional PID controller and another new controller. These results demonstrate that the proposed controller confirms better disturbance rejection, keeps the control quality in the wider operating range, reduces the frequency's transient response avoiding the overshoot and is more robust to uncertainties in the system.

Keywords: Load frequency control (LFC), multi objective optimization algorithm, SMES, Fuzzy sliding mode control.

© 2016 IAUCTB-IJSEE Science. All rights reserved

1. Introduction

Frequency is one of the stability conditions for large-scale power systems. In power systems, frequency is depending on active power. Any change in active power demand/generation at power systems is reflected throughout the system by a change in frequency so that if active power consuming increases in an area, the frequency of power systems will decrease and vice versa [1]. In multi-area power systems, frequency changes can lead to severe stability problems. To prevent such a situation, it is essential to design a load frequency control (LFC) systems that control the output active power of generator and tie line active power. In the conventional LFC, PI controllers are the most

commonly used ones. Several methods have been proposed in the literature to tune the gain of the PI controller [2]. To overcome the disadvantages of conventional PI controller, innovative control methods were recommended for the LFC such as optimal control [3–5], variable structure control [6], adaptive control [7,8] and robust control [9–11]. Nevertheless, these approaches are depending on either information about the system states or an efficient on-line identifier thus may be difficult to implement in practice. Furthermore, many stabilization techniques are used to efficiently mitigate oscillations by extending the conventional PI controller. In [12], an extended integral control

has been proposed to acquire zero steady-state error as well as having a limited overshoot in dynamic response after a step change in load. In [13,14], fuzzy PI controllers have been suggested for load frequency control of power systems. In the introduced works, the derivative gain does not exist in load frequency control owing to the effect of noise on its performance. However, investigations confirmed a positive effect of a differential feedback in LFC on system damping [15]. Thus, there is a compromise between a suitable damping and noise. To lessen the effect of environment noise, a different derivative structure with less effect noise was proposed [16]. From that day forward, researchers focused on load frequency controller of PID type. In [17], a PID load frequency controller tuning method for a single-machine infinite-bus (SMIB) system was proposed based on the PID tuning method proposed in [18,19], and the method is extended to two- area cases [20]. Among methods offered for the LFC, optimization algorithms are popular methods to adjust parameters of LFC so that different kind of algorithms such as particle swarm optimization (PSO) [21], genetic [22,23], bacteria foraging [24] have been proposed for this purpose so far. In all of these methods, parameters are optimized by the classical weighted-sum approach where the objective function is formulated as a weighted-sum of the objectives. But the problem lies in the correct selection of the weights to characterize the decision-makers preferences. In recent years, the multi-objective problems are used to find non-inferior (Pareto-optimal, non-dominated) solutions. The most widely used methods for generating such non-inferior solutions are the weighting method, ϵ -constraint method and weighed min-max method. The decision maker has to choose the best compromise solution from the obtained solution set. Literature review demonstrates that in most works proposed for the LFC [21-24], though area control errors converge to zero efficiently, however, the frequency and the tie-line power deviations take a relatively long time period. This means that a long settling time can be seen in the dynamic response of these signals. In this status, the governor system may not be able to control the frequency changes, because of its slow dynamic [25]. Thus, as an effective action overcomes the sudden load changes, an active power source with fast response like SMES units is good choice. Some papers have offered the application of an SMES in each area of a two-area system [26,27]. As foreseen, the frequency deviations and active power tie-line were efficiently damped out. However, from economic point of view, it is not achievable to place an SMES in every area of a multi-area interconnected power system. Therefore, an SMES with a large capacity located in one of the

areas where is available for the control of other interconnected areas was proposed [28]. Since the mitigation of frequency deviations was not in line with expectations, a combination of flexible AC transmission system (FACTS) devices such as solid-state phase shifters [28] and SSSC [29] with the SMES was proposed. By doing so, notwithstanding the satisfactory damping of oscillations and deviations, the economic feasibility is still a challenging problem for such an approach. In this study, a fuzzy sliding mode controller (FSMC) with integral-proportion-Derivative switching surface is proposed to control an SEMS for the power system load frequency control. To achieve a maximum damping of frequency deviations, this method is combined with PIDs tuned by a multi-objective optimization algorithm. The goal of design is to improve the dynamic response of power systems after load demand changes. In the proposed method, an adaptive fuzzy controller is utilized to mimic a feedback linearization control law. To compensate the compensation error between the feedback linearization and adaptive fuzzy controller, a hitting controller is developed. The Lyapunov stability theory is used to obtain an adaption law so that the closed-loop system stability can be guaranteed. Three separate objective functions are simultaneously minimized by the proposed approach in order to achieve an optimum LFC. The main motivation of using GA is for the reason that it deals simultaneously with a set of possible solutions (the so-called population) which allows the user to find several members of the population. Additionally, GAs are less susceptible to the shape or continuity of the Pareto front as they can easily deal with discontinuous and concave Pareto fronts, whereas these two issues are known problems with mathematical programming [30]. To select the best compromise solution from the obtained Pareto set, a fuzzy-based approach is used [30]. Simulation results are presented and compared with a conventional GA-PID controller and the results obtained from the tuning method of LFC proposed in [20].

2. Two-area load frequency control

Fig. 1 displays a standard block diagram of a two area interconnected power system [2]. This model includes a conventional PI controller that sets the turbine reference power of each area. The tie-line Power ΔP_{tie} flows throughout the tie-line between existing areas. To successfully control the frequency and active power generation, the supplementary frequency control should control and balance the power flow at the tie-line and also damp oscillations at the tie line. To achieve this goal, the easiest way is to combine the local frequency variation in each area

and the tie-line power variations together. This signal is named the area control error (ACE). In general, to

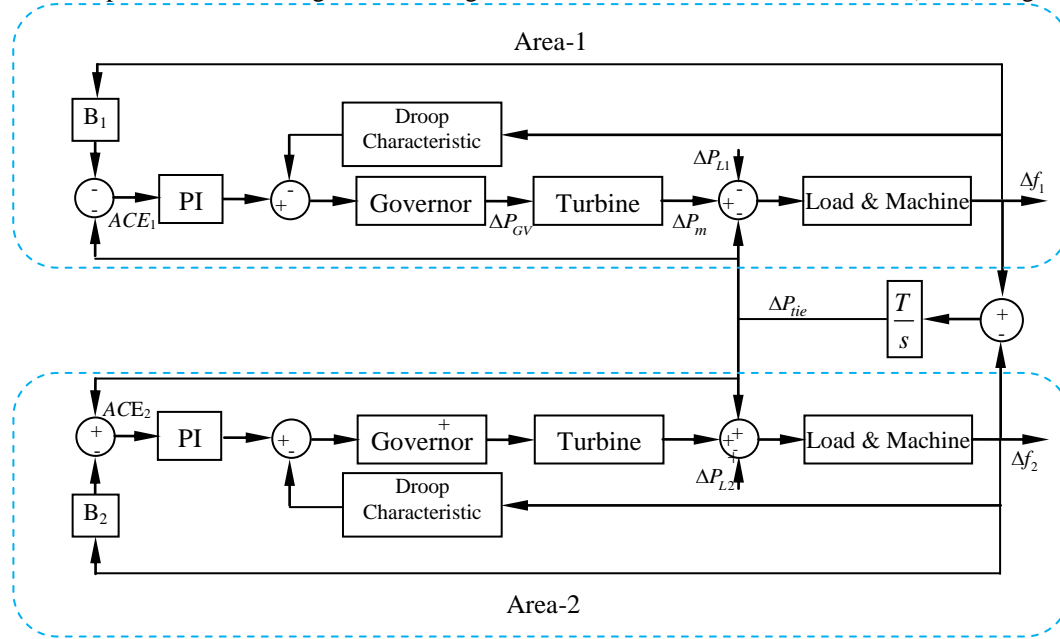


Fig. 1. Block diagram of a two area interconnected power system.

achieve a satisfactory operation of generating units, the frequency and tie-line power should be fixed on their scheduled values even though a load disturbance occurs and thus, $ACE=0$. In Fig. 1, each block is shown by the following transfer function.

- Steam turbine = $1/(T_T s + 1)$
- Load and machine = $1/(2Hs + D)$
- governor = $1/(T_g s + 1)$
- Droop characteristics of governor = $1/R$

where T_T and T_g are the turbine and governor time constants, respectively; H and D are the inertia coefficient of generator and ratio of load changes percentage to frequency changes percentage, respectively; ΔP_m and ΔP_{GV} are the incremental changes in the output mechanical power of turbine and governor valve position, respectively.

3. Overview of SMES

SMESs as a modern and new technology can store electrical power from the network within the magnetic field of a coil made of superconducting wire with near-zero loss of energy. Large values of energy can nearly instantaneously be stored and restored by SMESs. Therefore, the power system can release high levels of power within a fraction of a cycle to prevent a sudden loss in the line power. The SMES inductor-converter unit is composed of a dc super-conducting inductor, a type AC/DC converter and a step down transformer [31]. The reliability of a

SMES unit is higher than many other power storage devices, since all parts of a SMES unit are static. Ideally, when the superconducting coil is charging, the current will not fall and the magnetic energy can be stored indefinitely.

The schematic diagram of the arrangement of a thyristor controlled SMES unit is shown Fig. 2. By controlling the converter firing angle, the DC voltage appearing across the inductor can change continuously from a certain negative value to a positive value. The inductor is firstly charged to its rated current I_{d0} by using a small positive voltage. By disregarding the transformer and the converter losses, the DC voltage across the inductor is [31]:

$$E_d = 2V_{d0} \cos \alpha - 2I_d R_C \quad (1)$$

where α is the firing angle (in degrees); I_d is the current flowing through the inductor (in kA); R_C is the equivalent commutating resistance (in k Ω) and V_{d0} is the maximum circuit bridge voltage (in kV). Charging and discharging of the SMES unit can be controlled by changing the firing angle α .

In the LFC operation, the E_d is continuously controlled by the input signal to the SMES control loop. As stated in [31], to instantly react to the next load disturbance, the current of inductor must be rapidly reinstated to its nominal value after an electrical load disturbance.

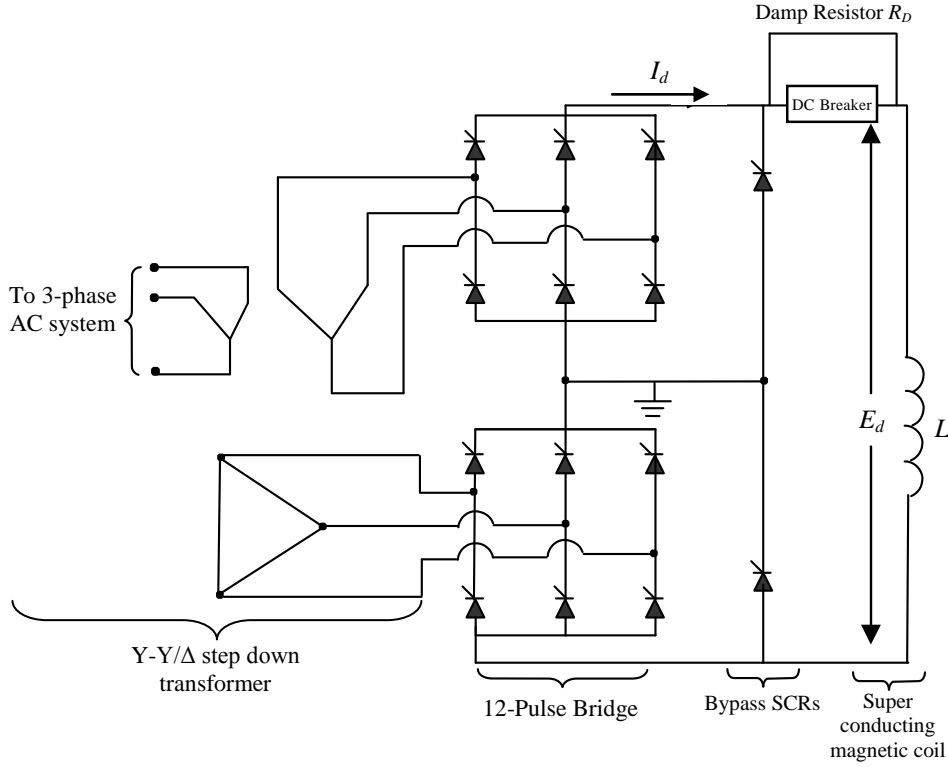


Fig. 2. SMES circuit diagram

To achieve this goal, the inductor current deviation (ΔI_d) is used as a negative feedback signal in the control loop of SMES. Accordingly, the converter voltage applied to the inductor (ΔE_d) and inductor current deviations (ΔI_d) can be written as follows:

$$\Delta E_d(s) = \frac{1}{1+sT_c} U_{FSMC}(s) - \frac{k_f}{1+sT_c} \Delta I_d(s) \quad (2)$$

$$\Delta I_d(s) = \frac{1}{sL} \Delta E_d(s) \quad (3)$$

where U_{FSMC} is the control effort of FSMC; T_c is the time constant of converter (in second); k_f is the feedback gain of ΔI_d in the SMES unit; L is the inductance value of super conducting magnetic coil (in H).

The output real power deviation of SMES unit is represented by:

$$\Delta P_{SM} = \Delta E_d \cdot \Delta I_d + \Delta E_d \cdot I_{d0} \quad (4)$$

The block diagram of the FSMC based SMES unit is shown in Fig. 3.

4. Sliding mode control

The dynamic of the power system is described as

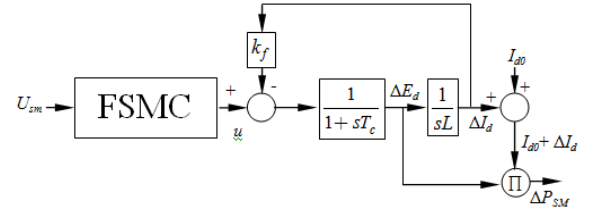


Fig. 3. Block diagram of the FSMC based SMES unit.

$$\ddot{x}(t) = f(x(t)) + Bu(t) + \gamma(t) \quad (5)$$

where $x(t) \in R^n$ is a state vector, $u(t) \in R^m$ is a control vector, $\gamma(t) \in R^n$ is a bounded signal that represents uncertainty or disturbance, $B \in R^n$ is a constant matrix, $f(x(t))$ is a map $x(t) \in R^n \rightarrow f(x(t)) \in R^n$ and t denotes time. The control objective is to find a suitable control law so that the trajectory state x can track a trajectory command x_d . Define a tracking error as

$$e = x - x_d \quad (6)$$

The first phase of sliding-mode control design is to choose a sliding surface which models the desired closed-loop performance in state variable space. Then, the controller should be designed in such a way that the system state trajectories are forced in the direction of the sliding surface and stay on it. Now, assume that an integral operation sliding surface is presented as

$$s(t) = k_1 e(t) + k_2 \int_0^t e(\tau) d\tau + k_3 \dot{e}(t) \quad (7)$$

where k_1 and k_2 are non-zero positive constants. If the system dynamic function is well-known, there is an ideal controller as:

$$u^* = -f(x) + \ddot{x}_d + k_1 \dot{e} + k_2 e \quad (8)$$

Substituting the ideal controller (8) into (5), we obtain

$$\ddot{e} + k_1 \dot{e} + k_2 e = 0 \quad (9)$$

If the control gains k_1 and k_2 are appropriately selected such that the characteristic polynomial of (9) is strictly Hurwitz, that is a polynomial whose roots lie strictly in the open left half of the complex plane, then it implies that $\lim_{t \rightarrow \infty} e(t) = 0$. Given that the system dynamic and the external load disturbance are always unknown or perturbed, the control law u^* is not implementable in practical applications. Therefore, an AFSMC system is used to mimic the control law in this paper.

5. The proposed approach

A) Strategy of control

The proposed strategy of control is composed of two separate parts: PID controllers tuned by a multi-objective optimization algorithm, a fuzzy sliding mode controller based SMES. The configuration of proposed control strategy for the LFC problem is depicted in Fig. 4. As seen in Fig. 4, the tie-line power flow deviations ΔP_{tie} is selected as the input signal to the control loop of SMES. According to Fig. 4, the tie line power flow deviations modulated by the SMES unit are appended to both areas simultaneously with different signs (+ and -). In the configuration depicted in Fig. 4, to achieve the control inputs u_1 and u_2 , the optimal PID controllers are used together with area control errors, ACE_1 and ACE_2 in (10) and (11), as the input signal, respectively.

$$ACE_1 = B_1 \cdot \Delta f_1 + \Delta P_{tie} \quad (10)$$

$$ACE_2 = B_2 \cdot \Delta f_2 + \Delta P_{tie} \quad (11)$$

In the control strategy, the control signals u_1 and u_2 are represented by:

$$u_1(t) = K_{p1} \cdot ACE_1(t) + K_{i1} \int_0^t ACE_1(\tau) d\tau + K_{d1} \frac{dACE_1(t)}{dt} \quad (12)$$

$$u_2(t) = K_{p2} \cdot ACE_2(t) + K_{i2} \int_0^t ACE_2(\tau) d\tau + K_{d2} \frac{dACE_2(t)}{dt} \quad (13)$$

To achieve the best dynamical response of power system shown in Fig. 4, optimal solutions of PID controllers are considered as an optimization problem and multi-objective optimization algorithm will be utilized to solve it.

B) FSMC system design

Structure of intelligent control system

Fig. 5 shows the block diagram of control system that is used to modulate the output power of SMES unit. The control system contains the blocks of sliding surface, fuzzy controller, adaption law, hitting controller and bound estimation. As seen in this figure, the inputs of sliding surface is error between the tie-line power flow deviation ΔP_{tie} and desired value ΔP_d , i.e. $U_{sm} = e = (\Delta P_{tie} - \Delta P_d)$. In this paper, ΔP_{tie} and ΔP_d are selected as trajectory command and trajectory state given in (6). The desired value of tie-line power flow deviation is selected to be zero, since this signal in steady-state and no disturbance conditions is zero. As shown in Fig. 5, the output of controller is

$$u = \hat{u}_{fz} + u_{vs} \quad (14)$$

where the fuzzy controller \hat{u}_{fz} is the head tracking controller to mimic the control law u^* and the hitting control u_{vs} is used to compensate the difference between the control law and the fuzzy controller. Moreover, as seen in Fig. 5, the output of the AFSMC after being clipped is summed with the exciter system's input. In disturbance conditions, the SMES unit regulates its output power based on the output of the AFSMC.

Description of fuzzy controller

If α_i is selected as an adjustable parameter, we can write

$$u_{fz}(s, \alpha) = \alpha^T \xi \quad (15)$$

where $\alpha = [\alpha_1; \alpha_2; \dots; \alpha_m]^T$ is a parameter vector and $\xi = [\xi_1; \xi_2; \dots; \xi_m]^T$ is a regressive vector with ξ_i described by

$$\xi_i = \frac{w_i}{\sum_{j=1}^m w_j} \quad (16)$$

where w_i is the firing weight of the i th rule. Regarding the universal approximation theorem [32],

there is an optimal fuzzy control system $u_{fz}^*(s, \alpha^*)$ in the form of (14) such that

$$u^*(t) = u_{fz}^*(s, \alpha^*) + \varepsilon = \alpha^{*T} \zeta + \varepsilon \quad (17)$$

where ε is the approximation error and is supposed to be limited by $|\varepsilon| < E$. Using a fuzzy control system $\hat{u}_{fz}(s, \hat{\alpha})$ to approximate $u^*(t)$

$$\hat{u}_{fz}(s, \hat{\alpha}) = \hat{\alpha}^T \zeta \quad (18)$$

where $\hat{\alpha}$ is the estimated vector of α^* . By substituting (17) into (5), it is shown that

$$\ddot{x}(t) = f(x(t)) + B[\hat{u}_{fz} + u_{vs}] + \gamma(t) \quad (19)$$

After some straightforward manipulation, the error equation governing the closed-loop system can be obtained from (7), (8) and (18) as follows:

$$k_1 e(t) + k_2 \int_0^t e(\tau) d\tau + k_3 \dot{e}(t) = B[\hat{u}_{fz} + u_{vs} - u^*] = \dot{s}(t) \quad (20)$$

And, \tilde{u}_{fz} is denoted as

$$\tilde{u}_{fz} = \hat{u}_{fz} - u^* = \hat{u}_{fz} - [u_{fz}^* + \varepsilon] \quad (21)$$

To simplify discussion, define $\tilde{\alpha} = \hat{\alpha} - \alpha^*$ to acquire a rephrased form of (20) via (16) and (17) as

$$\tilde{u}_{fz} = \tilde{\alpha}^T \zeta - \varepsilon \quad (22)$$

In fact, the basic idea of Lyapunov stability theory is the mathematical extension of a fundamental physical observation: if the total energy of a system is continuously dissipated, then the system must finally stay in equilibrium point. Thus,

the stability of a system is the descent variation of an energy function (Lyapunov function) for introducing a suitable control law and associated adaptation rules. To force $s(t)$ and $\tilde{\alpha}$ tend to zero, define a Lyapunov function as:

$$V_a(t) = \frac{1}{2} s^2(t) + \frac{B}{2\eta_1} \tilde{\alpha}^T \tilde{\alpha} \quad (23)$$

where η_1 is a positive constant. Differentiating (22) with respect to time, we can obtain

$$\begin{aligned} \dot{V}_a(t) &= s(t)\dot{s}(t) + \frac{B}{2\eta_1} \tilde{\alpha}^T \dot{\tilde{\alpha}} = s(t)B(\hat{u}_{fz} + u_{vs} - u^*) + \frac{B}{2\eta_1} \tilde{\alpha}^T \dot{\tilde{\alpha}} \\ &= s(t)B(\tilde{\alpha}^T \zeta + u_{vs} - \varepsilon) + \frac{B}{2\eta_1} \tilde{\alpha}^T \dot{\tilde{\alpha}} \\ &= B\tilde{\alpha}^T \left(s(t)\zeta + \frac{1}{\eta_1} \dot{\tilde{\alpha}} \right) + s(t)B(u_{vs} - \varepsilon) \end{aligned} \quad (24)$$

This shows that $\dot{V}(t)$ is a negative semi-definite function. Define the following equation

$$Q(t) = (E - |\varepsilon|) |s(t)| B \leq -\dot{V}_a(t) \quad (25)$$

Since $V_a(t)$ is bounded and $V_a(t)$ is non-increasing and bounded, then

$$\int_0^t Q(\tau) d\tau \leq V_a(t_1) - V_a(t_2) < \infty \quad (26)$$

Moreover, since is bounded by Barbalat's Lemma [33], $\lim_{t \rightarrow \infty} Q(t) = 0$. That is, $s(t) \rightarrow 0$ as $t \rightarrow \infty$. Accordingly, the stability of the AFSMC can be guaranteed.

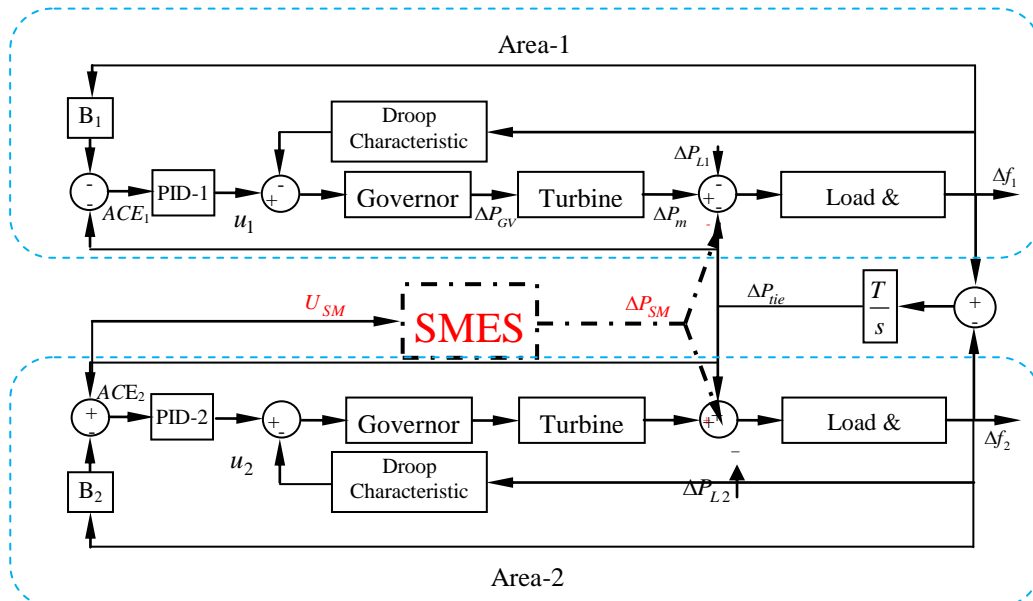


Fig. 4. Control configuration for the LFC problem along with the SMES unit.

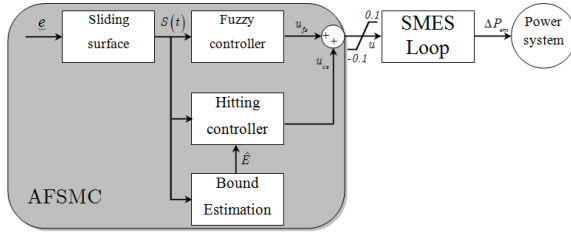


Fig. 5. The block diagram of AFSMC

To implement AFSMC system, the approximation error should be bounded. However, the bound of approximation error E cannot be measured simply for practical applications in industry. If E is chosen too large, we will observe large chattering in the control effort. If E is chosen too small, the control system may be destabilized. To surmount the requirement for the bound of approximation error, we use the AFSMC system with bound estimation. Replacing E by $\hat{E}(t)$ in (25), we have:

$$u_{vs} = -\hat{E}(t) \operatorname{sgn}(s(t)) \quad (27)$$

Where $\hat{E}(t)$ is the estimated bound value of the approximation error. Consider the following estimated error as

$$\tilde{E}(t) = \hat{E}(t) - E \quad (28)$$

To force the $s(t)$, $\tilde{\alpha}$ and $\tilde{E}(t)$ tend to zero, define the following Lyapunov function.

$$V_b(t) = \frac{1}{2} s^2(t) + \frac{B}{2\eta_1} \tilde{\alpha}^T \tilde{\alpha} + \frac{B}{2\eta_2} \tilde{E}^2 \quad (29)$$

where η_2 is a positive constant.

Differentiating (31) with respect to time and using (34) and (29), we can obtain

$$\begin{aligned} \dot{V}_b(t) &= s(t)\dot{s}(t) + \frac{B}{2\eta_1} \tilde{\alpha}^T \dot{\tilde{\alpha}} + \frac{B}{2\eta_2} \tilde{E} \dot{\tilde{E}} \\ &= B\tilde{\alpha}^T \left(s(t)\zeta + \frac{1}{\eta_1} \dot{\tilde{\alpha}} \right) + s(t)B(u_{vs} - \varepsilon) + \frac{B}{2\eta_2} \tilde{E} \dot{\tilde{E}} \\ &= -\hat{E}(t) |s(t)| B - \varepsilon s(t) B + \frac{B}{\eta_2} [\hat{E}(t) - E] \dot{\tilde{E}}(t) \end{aligned} \quad (30)$$

To achieve $\dot{V}_b(t) \leq 0$, the following estimation law is used.

$$V_b(t) = \frac{1}{2} s^2(t) + \frac{B}{2\eta_1} \tilde{\alpha}^T \tilde{\alpha} + \frac{B}{2\eta_2} \tilde{E}^2 \quad (31)$$

Then we can rewrite (29) as

Using Barbalat's lemma [33], we can conclude that $s(t) \rightarrow 0$ as $t \rightarrow \infty$. In summary, the AFSMC system with bound estimation is given in (14), where \hat{u}_{ε} is presented in (17) with the parameters $\hat{\alpha}$ updated by (24); u_{vs} is presented in (27) with the parameter \hat{E} updated by (31). By employing this estimation law, the convergence of AFSMC system with bound estimation can be guaranteed.

C) Optimization problem

It is worth mentioning that the PID controllers are designed to improve the dynamic performance of the power system after a load demand change by removing the frequency oscillations and steady-state error. The objectives can be formulated as the minimization of multi-objective functions J given by:

$$J = (J_1, J_2, J_3) \quad (32)$$

Where

$$J_1 = \int_0^t \tau |\Delta f_1(\tau)| d\tau \quad (33)$$

$$J_2 = \int_0^t \tau |\Delta f_2(\tau)| d\tau \quad (34)$$

$$J_3 = \int_0^t \tau |\Delta P_{tie}| d\tau \quad (35)$$

Where t is the simulation period; Δf_1 and Δf_2 are the frequency deviations in area 1 and 2; ΔP_{tie} is the tie-line power.

6. Multi objective optimization algorithm

A) Multi-objective optimization problem and Pareto solutions

A multi-objective optimization problem (MOP) can optimize several objectives. So, an MOP is different from a single-objective optimization problem (SOP). In case of single-objective optimization problems, the purpose is to acquire the best single design solution; while in MOPs with several and probably incompatible objectives, there usually exists no single optimal solution. So, the decision maker is obligated to select a solution from a finite set by making compromises. A suitable solution should provide for acceptable performance over all objectives [30]. A general formulation of an MOP contains numerous objectives with numerous inequality and equality constraints. In a mathematical way, the problem can be represented as follows [30]:

$$\begin{aligned}
& \text{minimize/maximize } f_i(x) \quad \text{for} \\
& i=1,2,\dots,n. \\
& \text{Subject to} \\
& g_j(x) \leq 0 \quad j=1,2,\dots,J \\
& h_k(x) \leq 0 \quad k=1,2,\dots,K
\end{aligned} \tag{36}$$

where $f_i(x)=\{f_1(x),\dots,f_n(x)\}$; n denotes the number of objectives; $x=\{x_1,\dots,x_p\}$ is a vector of decision variables; p denotes the number of decision variables.

The MOP can be solved by two approaches. The first one is the classical weighted-sum approach. In this approach, the objective function is formulated as a weighted-sum of the objectives. But the problem lies in the correct selection of the weights or utility functions to characterize the decision-makers preferences. The second approach called Pareto-optimal solution can be used to solve this problem. The MOPs usually have no unique or perfect solution, but a set of non-dominated, alternative solutions, known as the Pareto-optimal set. Assuming a minimization problem, dominance is defined as follows:

$$\begin{aligned}
& \text{A vector } \mathbf{u}=(u_1,\dots,u_n) \text{ is said to be} \\
& \text{dominate } \mathbf{v}=(v_1,\dots,v_n) \text{ if and only :} \\
& \forall i \in \{1,\dots,n\}, u_i \leq v_i \wedge \exists i \in \{1,\dots,n\}; u_i < v_i
\end{aligned} \tag{37}$$

A solution $x_u \in u$ is said to be Pareto-optimal if and only if there is no $x_v \in u$ for which $\mathbf{v}=\mathbf{f}(x_v)=(v_1,\dots,v_n)$ dominates $\mathbf{u}=\mathbf{f}(x_u)=(u_1,\dots,u_n)$.

Pareto-optimal solutions are also called efficient, non-dominated, and non-inferior solutions. The corresponding objective vectors are simply called non-dominated. The set of all non-dominated vectors is known as the non-dominated set, or the trade-off surface, of the problem. A Pareto-optimal set is a set of solutions that are non-dominated with respect to each other. While moving from one Pareto solution to another, there is always a certain amount of sacrifice in one objective to achieve a certain amount of gain in the other. The elements in the Pareto set has the property that it is impossible to further reduce any of the objective functions, without increasing, at least, one of the other objective functions. A complete explanation about Pareto-optimal solution can be found in [27].

B) GA method for generating Pareto solutions

The ability to handle complex problems, involving features such as discontinuities, multi-modality, disjoint feasible spaces and noisy function evaluations reinforces the potential effectiveness of GA in optimization problems. Although, the conventional GA is also suited for some kinds of multi-objective optimization

problems, it still difficult to solve those multi-objective optimization problems in which the individual objective functions are in the conflict condition.

Being a population-based approach; GA is well suited to solve MOPs. A generic single-objective can be easily modified to find a set of multiple non-dominated solutions in a single run. The ability of GA to simultaneously search different regions of a solution space makes it possible to find a diverse set of solutions for difficult problems with non-convex, discontinuous, and multi-modal solutions spaces. The crossover operator of GA exploits structures good solutions with respect to different objectives to create new non-dominated solutions in unexplored parts of the Pareto front. In addition, most multi-objective GA does not require the user to prioritize, scale, or weigh objectives. Therefore, GA has been the most popular heuristic approach to multi-objective design and optimization problems.

Pareto-based fitness assignment was first proposed by Goldberg [26], the idea being to assign equal probability of reproduction to all non-dominated individuals in the population. The method consisted of assigning rank 1 to the non-dominated individuals and removing them from contention, then finding a new set of non-dominated individuals, ranked 2, and so forth. In the present study, before finding the Pareto-optimal individuals for the current generation, the Pareto-optimal individuals from the previous generation are added. The number of Pareto-optimal individuals is limited, when it exceeds the defined number. This is done by calculating a function of closeness between the individuals given as below:

$$D(x) = (\min |x - x_i| + \min |x - x_k|) / 2 \tag{38}$$

where $x \neq x_i \neq x_k$ are individuals on the Pareto-surface. The individual with smaller value of D (distance to the other points) is removed. This process continues until the desired number of points is achieved. Besides limiting the number of points this also helps to keep the diversity of the Pareto-set and obtain better spread surface. How to limit the Pareto-optimal set has briefly been explained in [25].

7. Simulations and discussions

In this paper, MATLAB is used to implement the optimization algorithm and to simulate the cases. At this time, the performance of the proposed method is evaluated under different disturbances. To validate the effectiveness of the proposed approach in damping the power system oscillations, the results obtained from the AFSMC are compared with other controllers proposed in [20] and [31]. If the values of k_1 , k_2 and k_3 are properly selected, the

desired system dynamics such as rise time, overshoot, and settling time can be easily achieved. Moreover, the gains η_1 and η_2 are chosen to achieve the best transient responses by trial and error in the experimentation taking into consideration the constraint of stability and the control effort. The parameters used in the AFSMC are given in Table 1.

Table.1.
The parameters used in the AFSMC.

Parameter	η_1	η_2	k_1	k_2	k_3
	10	0.5	17	17	3

C) Generation of Pareto solution set

In this paper, Pareto solutions are generated by GA for the PID gains in each area so as to minimize the objective function J . To apply GA, a number of parameters should be determined. A proper selection of the parameters has an impact on the speed of convergence of the algorithm. The parameters used for the multi-objective genetic algorithm (MGA) are provided in Table 2. The objective function is evaluated for each individual by simulating the example power system, considering a $\Delta P_{L1}=0.2$ at $t=0$. The optimization is terminated by the pre-specified number of generations. In this paper, the number of individuals in the Pareto-optimal set is selected 13. In addition, the best compromise solution from the obtained Pareto set is chosen by a Fuzzy-based approach. The j th objective function of a solution in a Pareto set J_j is represented by a membership function μ_j defined as [30]:

$$\mu_j = \begin{cases} 1, & J_j \leq J_j^{\min} \\ \frac{J_j^{\max} - J_j}{J_j^{\max} - J_j^{\min}}, & J_j^{\min} < J_j < J_j^{\max} \\ 0 & J_j \geq J_j^{\max} \end{cases} \quad (39)$$

where J_j^{\min} and J_j^{\max} denote the maximum and minimum values of the j th objective function, respectively.

For each solution i , the membership function can be obtained from the following equation.

$$\mu^i = \frac{\sum_{j=1}^n \mu_j^i}{\sum_{i=1}^m \sum_{j=1}^n \mu_j^i} \quad (40)$$

where n and m denote the number of objectives functions and the number of solutions, respectively. The solution possessing the maximum value of μ^i is the best compromise solution. Table 2 presents the obtained Pareto solution set; values of

objective functions (J_1 , J_2 and J_3) associated with the Pareto solutions and the membership function values of each solution. In Table 3, Pareto solution set are shown by MGA-x; $x=1, 2, \dots, 11$. As seen in Table 3, maximum membership function value belongs to MGA-1 ($\mu^9=0.1149$). Hence, results obtained in MGA-9 are the best compromise solution and should be selected as optimal gains of PID controllers.

Table.2.

Parameters used in multi-objective genetic optimization	
Parameter	Value/Type
Maximum generations	100
Population size	50
Mutation rate	0.01
Number of Pareto-surface individuals	11

D) Simulation results

To demonstrate the impressiveness of the proposed design approach, simulations are performed for the example power system displayed in Fig. 4. In order to verify the proposed approach, the results obtained from the proposed approach are compared with the responses obtained from [20] and [31].

The frequency deviations Δf_1 , Δf_2 , tie-line power flow and ΔP_{sm} for $\Delta P_{L1}=0.2$ are shown in Figs. 6 (a-d). It is clear from these figures that the proposed method provides a better dynamical response compared to the conventional LFC and method proposed in [20] in damping deviations effectively and reducing settling time. Hence compared to the other methods, proposed approach greatly increases the system stability and improves the damping characteristics of the interconnected power system.

In fig 7 is shown a disturbance signal is added to the control signal to evaluate the robustness of controller against disturbance. The disturbance signal is a voltage pulse added to U_T after settling time (I. e., time interval between 6s and 7s). It is supposed that the amplitude of disturbance pulse is 1v and the pulse duration is 1s. Figure 7 depicts the structure of the proposed controller.

For the second simulation, a 20% increase in demand of area 2 is applied at $t=0$. The frequency deviations Δf_1 , Δf_2 , tie-line power flow and ΔP_{sm} for this disturbance are shown in Figs. 7 (a-d). As seen in these figures, the proposed approach has again provided a better dynamic response than other methods. A comparative study between the proposed methods is provided in Table 4. As seen in this Table, the proposed provides a less settling time compared to the other methods.

Table.3.
Pareto solutions, objective functions and value of memberships.

Solution	PID-1			PID-2			J_1	J_2	J_3	μ^i
	K_p	K_i	K_d	K_p	K_i	K_d				
MGA-1	3.0000	3.0000	1.7500	3.0000	3.0000	3.0000	0.0588	0.0663	0.0765	0.0828
MGA-2	3.0000	2.0000	1.7500	3.0000	3.0000	2.0000	0.0705	0.0692	0.0530	0.1085
MGA-3	0.1660	0.2802	0.6095	1.5184	0.5779	0.5746	0.4742	0.4746	0.0423	0.0472
MGA-4	0.2634	0.2171	0.3935	1.6481	0.6019	0.8858	0.5172	0.5179	0.0403	0.0416
MGA-5	3.0000	2.9416	1.7500	3.0000	3.0000	2.0000	0.0596	0.0637	0.0584	0.1037
MGA-6	0.6563	0.9858	1.0097	1.9401	2.0482	1.9047	0.1412	0.1408	0.0428	0.1072
MGA-7	1.2886	1.8956	1.3678	2.7521	2.8336	1.9419	0.0885	0.0905	0.0461	0.1128
MGA-8	2.9867	2.9800	1.5115	2.8698	2.9876	1.4537	0.0500	0.0770	0.0754	0.0833
MGA-9	2.8820	2.2866	1.6631	2.4331	2.9474	1.2892	0.0660	0.0716	0.0475	0.1149
MGA-10	2.7500	2.9219	2.0000	3.0000	3.0000	3.0000	0.0634	0.0664	0.0562	0.1057
MGA-11	2.9704	2.8578	1.4844	2.7066	2.9491	1.3172	0.0582	0.0789	0.0673	0.0922

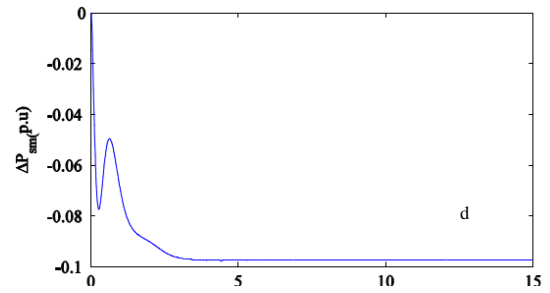
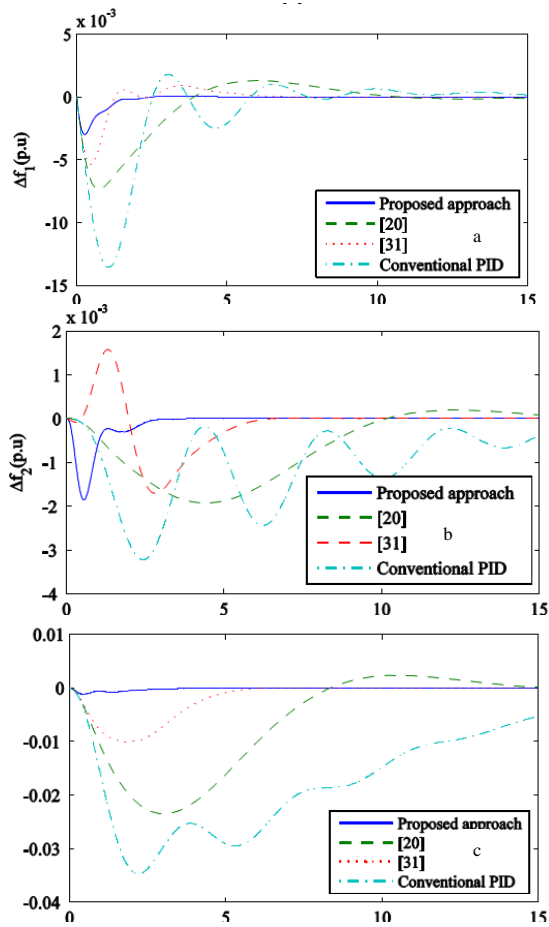
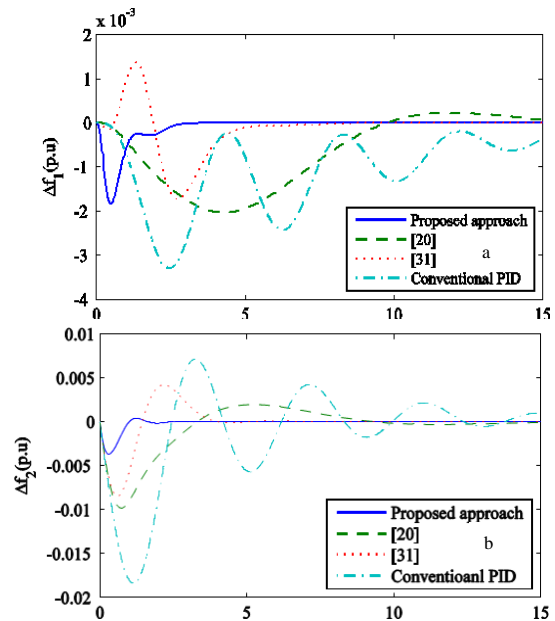


Fig. 6. Responses of power system to a $\Delta PL2=0.2$ applied to area-1; (a) frequency deviation in areas 1 (b) frequency deviation in area 2 (c) tie-line power flow deviation; (d) the output of SMES unit.



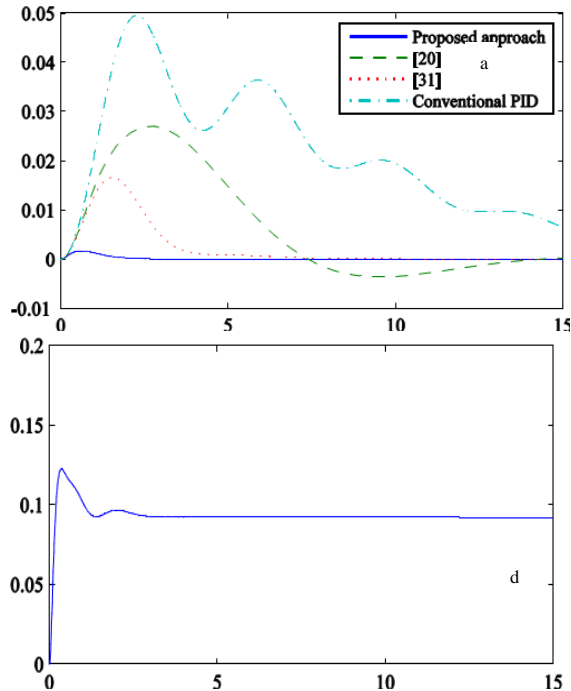


Fig. 7. Responses of power system to a $\Delta PL_2=0.2$ applied to area-1; (a) frequency deviation in areas 1 (b) frequency deviation in area 2 (c) tie-line power flow deviation; (d) the output of SMES unit.

Simulation results show that the performance of the multi-objective genetic algorithm is better than the other methods. In all cases the damping of interconnected power system following the disturbance has improved significantly. It should be noted that in this example the inherent damping of the system was chosen relatively low and the system becomes unstable under contingencies.

Table.4.
The parameters used in the AFSSMC.

Type of method	Settling time (s)					
	$\Delta P_{L1}=0.2$			$\Delta P_{L2}=0.2$		
	Δf_1	Δf_2	ΔP_{tie}	Δf_1	Δf_2	ΔP_{tie}
Proposed approach	5.94	6.01	5.70	7.41	3.77	6.81
Method proposed in [31]	6.12	6.11	5.73	7.68	3.83	6.89
Method proposed in [20]	12.68	19.03	19.03	18.69	15.12	15.36
Conventional PID	14.35	22.97	24.70	22.85	19.30	23.24

8. Conclusion

In this paper, a combination of a fuzzy sliding mode controller (FSMC) with integral-proportion-Derivative switching surface based SEMS and PID tuned by a multi-objective optimization algorithm

is proposed to solve the load frequency control in power systems. In order to improve the dynamical response of an interconnected power system, in the proposed approach, a fuzzy sliding mode controller is added to the control loop of an SMES. Obtaining the optimal PID controller problem is formulated into a multi-objective optimization problem. A Pareto set of global optimal solutions to the given multi-objective optimization problem is generated by a genetic algorithm (GA)-based solution technique. The best compromise solution from the generated Pareto solution set is selected by using a fuzzy-based membership value assignment method. Simulations are presented and compared with conventional PID controller and other new controllers. These results demonstrate that the proposed controller confirms better disturbance rejection, keeps the control quality in the wider operating range, reduces the frequency's transient response avoiding the overshoot and is more robust to uncertainties in the system.

Appendix

SMES loop control:

$$T_c=0.03, I_{d0}=20\text{kA}, L=3\text{H}, \\ k_f=0.001$$

The system parameters are as follows (frequency=60Hz, MVA base=1000) [2]:

Area #1: $H=5, D=0.6, T_g=0.2, T_T=0.5, R=0.05, B_1=20.6$.

Area #2: $H=4, D=0.9, T_g=0.3, T_T=0.6, R=0.0625, B_2=16.9$.

Acknowledgment

This work was supported by Islamic Azad University of Parand branch. The authors would like to thank them for their unwavering support.

References

- [1] Kundur P. Power system stability and control. McGraw-Hill; 1994.
- [2] Saadat H. Power system analysis. McGraw-Hill; 1999.
- [3] F. Liu, Y.H. Song, J. Ma, S. Mei and Q. Lu, "Optimal load-frequency control in restructured" IEE Proc.-Gener. Transm. Distrib. Vol. 150, No. 1, 2003.
- [4] Cavin RK, Budge MC, Rasmussen P. "An optimal linear system approach to load frequency control", IEEE Trans 1971; PAS 90, 1971.
- [5] Calovic M. "Linear regulator design for a load and frequency control theory", IEEE Trans, Vol.91,1972.
- [6] Chan WC, Hsu YY. "Automatic generation control of interconnected power systems using variable-structure controller", IEE Proc 1981, Vol. 128, 1981.
- [7] Ashraf Mohamed Hemeida, "Wavelet neural network load frequency controller", Energy Conversion and Management, Vol. 46, No. 9-10, 2005.
- [8] Y. Oysal, A. S. Yilmaz, E. Koklukaya, "A dynamic wavelet network based adaptive load frequency control in

- power systems", *Electrical Power and Energy Systems*, Vol. 27, No. 1, 2005.
- [9] Wang ZQ, Sznaier M. "Robust control design for load frequency control using synthesis", In: *Southcon/94, Conference Record, Orlando, FL, USA; 1994.*
- [10] Ray G, Prasad AN, Prasad GD. "A new approach to the design of robust load-frequency controller for large scale power systems", *Elect Power Syst Res*, Vol. 51, 2002.
- [11] Azzam M. "Robust automatic generation control", *Energy Convers Manag*, Vol. 40, 1997.
- [12] Moon YH, Ryu HS, Lee JG, Song KB, Shin MC. "Extended integral control for load frequency control with the consideration of generation-rate constraints", *Elect Power Energy Syst*, Vol. 24, 2002.
- [13] Talaq J, Al-Basri F. "Adaptive fuzzy gain scheduling for load frequency control", *IEEE Trans. Power Syst*, Vol. 14, 1999.
- [14] Hossain MF, Takahashi T, Rabbani MG, Sheikh MRI, Anower M. "Fuzzy- proportional integral controller for an AGC in a single area power system", In: *Proceedings of 4th international conference on electrical and computer engineering. Bangladesh: ICECE, Dhaka; 2006.*
- [15] Moon YH, Ryu HS, Choi BK, Kook HJ. "Improvement of system damping by using the differential feedback in the load frequency control", In: *Proceedings of the IEEE PES 1999 winter meeting; 1999.*
- [16] Moon YH, Ryu HS, Lee JG, Kim S. "Power system load frequency control using noise-tolerable PID feedback", In: *Proceedings IEEE international symposium on industrial electronics (ISIE) 2001, vol. 3, 2001.*
- [17] Khodabakhshian A, Golbon N. "Unified PID design for load frequency control", In: *Proceedings of 2004 IEEE international conference on control applications (CCA). Taipei, Taiwan; 2004.*
- [18] Poulin E, Pomerleau A. "PID tuning for integrating and unstable processes", *IEE Proc Control Theory Appl*, Vol. 143, No. 5, 1996.
- [19] Poulin E, Pomerleau A. "Unified PID design method based on a maximum peak resonance specification", *IEE Proc Control Theory Appl*, Vol. 146, No. 6, 1997.
- [20] Khodabakhshian A, Edrisi M. "A new robust PID load frequency controller", *Control Eng. Pract*, Vol. 16, 2008.
- [21] H. Gozde, M. C. Taplamacioglu., "Automatic generation control application with craziness based particle swarm optimization in a thermal power system", *Elect. Power and Energy Syst*, Vol. 33, No.1, 2011.
- [22] Praghnessh Bhatt, Ranjit Roy, S.P. Ghoshal, "GA/particle swarm intelligence based optimization of two specific varieties of controller devices applied to two-area multi-units automatic generation control", *Electrical Power and Energy Systems*, Vol. 32, 2010.
- [23] F. Daneshfar H. Bevrani, " Load – frequency control: a G A-based multi-agent reinforcement learning", *IET Gener. Transm. Distrib*, Vol. 4, No. 1, 2010.
- [24] E.S. Ali, S.M. Abd-Elazim., Bacteria foraging optimization algorithm based load frequency controller for interconnected power system, *Elect. Power and Energy Syst*, Vol. 33, 2011.
- [25] Jaleeli N, Ewart DN, Fink LH. "Understanding automatic generation control", *IEEE Trans Power Syst*. Vol. 7, No. 3, 1992.
- [26] S.C. Tripathy, et al., " Adaptive Automatic Generation Control with Superconducting Magnetic Energy Storage in Power Systems ", *IEEE 'Prana. on Energy Conversion*, Vol. 7 , No. 3, 1992.
- [27] H. Shayeghi, A . Jalili, H.A. Shayanfar, " A robust mixed H_2/H_∞ based LFC of a deregulated power system including SMES", *Energy Conversion and Management*, Vol. 49, No. 10, 2008.
- [28] I. Ngamroo, Y. Mitani and K. Tsuji, " Application of SMES Coordinated with Solid-state Phase Shifter to Load Frequency Control", *IEEE Transactions on applied superconductivity*, Vol. 9, No. 2, 1999.
- [29] Praghnessh Bhatt, Ranjit Roy, S.P. Ghoshal, "Comparative performance evaluation of SMES–SMES, TCPS–SMES and SSSC–SMES controllers in automatic generation control for a two-area hydro–hydro system", *International Journal of Electrical Power & Energy Systems*, Vol. 33, No. 10, 2011.
- [30] Sidhartha Panda, "Multi-objective evolutionary algorithm for SSSC-based controller design", *Electric Power Systems Research* , Vol. 79, No. 6 , 2009.
- [31] Farahani, M., & Ganjefar, S. Solving LFC problem in an interconnected power system using superconducting magnetic energy storage, Vol 487, 2013.
- [32] L.X. Wang, *Adaptive Fuzzy Systems and Control: Design and Stability Analysis*, Prentice-Hall, Englewood Cliffs, NJ, 1994.
- [33] J.J.E. Slotine, W.P. Li, *Applied Nonlinear Control*, Prentice-Hall, Englewood Cliffs, NJ, 1991.